Research Square

Preprints are preliminary reports that have not undergone peer review.
They should not be considered conclusive, used to inform clinical practice,
or referenced by the media as validated information.

Modular magnetic recyclable dual-Escherichia coli cell factory with in situ UDP-glucose cofactor regeneration for high-efficiency green biosynthesis of isovitexin

Shuangqing Fu
Hebei University
Chao Zhang
Hebei University
Shuo Ma
Hebei University
Yujie Yuan
Hebei University
Wei Li
Hebei University
Honglei Zhang
zhanghonglei@hbu.edu.cn
Hebei University

Research Article

Keywords: Microbial cell factory, Isovitexin, C-glycosyltransferase, Modular whole-cell biocatalysis, Dual-strain cascade catalysis, In situ UDP-glucose cofactor regeneration, Magnetic hydrogel cell immobilization

Posted Date: July 23rd, 2026

DOI: https://doi.org/10.21203/rs.3.rs-10330075/v1

License: This work is licensed under a Creative Commons Attribution 4.0 International License. Read Full License

Additional Declarations: No competing interests reported.

Version of Record: A version of this preprint was published at Microbial Cell Factories on October 13th, 2026. See the published version at https://doi.org/10.1186/s12934-026-03140-5.

Abstract

Background

Flavone C-glycoside isovitexin exhibits potent antioxidant, anti-inflammatory and neuroprotective biological activities. Its existing biomanufacturing strategies are limited to low-yield plant extraction or purified free-enzyme cascade catalysis, which are plagued by expensive protein purification steps, absent endogenous cofactor circulation, and single-use non-recyclable biocatalysts. Recombinant whole-cell microbial cell factories offer a sustainable substitute, yet magnetically retrievable modular dual-strain chassis integrated with in situ UDP-glucose regeneration for isovitexin C-glycosylation biosynthesis have rarely been reported.

Results

In this work, we fabricated a magnetically separable modular dual-*Escherichia coli* cell factory via co-immobilization of two complementary engineered strains in Fe_3O_4-incorporated sodium alginate-polyvinyl alcohol-chitosan (SA-PVA-CS) ternary composite hydrogel microspheres. One strain expressed MBP-fused C-glycosyltransferase WjGT1 to catalyze apigenin C-glucosylation, while the other produced sucrose synthase SuSyAc to drive closed-loop intracellular UDP-glucose cofactor regeneration. Of three screened CGT enzymes, MBP-WjGT1 delivered the maximum soluble protein yield of 374 μg per mg wet cell and enabled 98.3% conversion of apigenin. Validated by UDP concentration gradient assays, the dual-strain cascade pathway fully sustained cofactor self-supplementation without external UDP addition under optimized parameters (WjGT1:SuSyAc mass ratio = 99.5:0.5, 10 mM sucrose, 5% DMSO, 0.5 mM apigenin). After 16 h bioconversion, 98.5% apigenin conversion and an isovitexin titer of 212.6 mg/L were achieved. The magnetic immobilized cell factory retained 80% catalytic activity compared with free dual whole-cell catalysts, and preserved 64% of its initial conversion capacity over seven successive magnetic recovery batches.

Conclusions

This modular magnetically recyclable dual-*E. coli* cell factory bypasses tedious enzyme purification and achieves autonomous cofactor recycling, constructing an economical, eco-friendly and reusable biomanufacturing platform for green isovitexin production. Moreover, this co-immobilization chassis can be generalized for scalable biosynthesis of various flavonoid C-glycosides, offering a robust engineering blueprint for developing industrial microbial cell factories targeting natural flavonoid compounds.

Background

Isovitexin (apigenin-6-C-glucoside), a prototypical bioactive flavone C-glycoside, occurs at trace levels in legumes, cereals, fruits, and medicinal herbs [1, 2]. Its architecture comprises an apigenin aglycone (2phenylchromen4one) scaffold C-glycosidically linked to glucose at the C6 position of the A ring—a linkage conferring resistance to acid and enzymatic hydrolysis. This distinctive hydroxylation pattern underpins potent antioxidant activity and supports the translational potential of isovitexin as an anti-inflammatory, anti-hyperglycemic, and neuroprotective candidate for Alzheimer's disease management [3–6]. Current industrial sourcing relies on plant extraction, a workflow fundamentally misaligned with scalable biomanufacturing due to intrinsically low native titers, batch-to-batch variability driven by germplasm and seasonality, laborious downstream processing, and high production costs [7–9]. To bypass these limitations, synthetic biology efforts have pivoted toward cell-free enzymatic cascades for flavonoid C-glycosylation [10, 11]. Pioneering studies engineered two-enzyme systems coupling a C-glycosyltransferase (CGT) with a sucrose synthase (SuSy) to achieve one-pot C-glucosylation of apigenin. Pei et al. reported a Gt6CGT–GmSUS cascade converting 1.0 mM apigenin/luteolin into C-glycosides at 94.7% molar yield [12], whereas Qiu et al. deployed a TcCGT–SuSy pair to synthesize isovitexin from 2 mM apigenin, attaining 97.3% conversion but a modest titer of 50 mg/L [13]. While these cell-free platforms benefit from exquisite substrate specificity and mild reaction conditions, their industrial translation remains constrained by three longstanding bottlenecks that microbial cell factories are inherently positioned to resolve: (i) costly, multistep chromatographic purification of recombinant enzymes; (ii) high upstream protein production burdens; and (iii) the lack of economically viable, self-sustaining cofactor regeneration systems in vitro.

Whole-cell biocatalysis has rapidly emerged as a compelling alternative to cell-free cascades, establishing itself as a central paradigm for sustainable microbial cell factories. Engineered microbes function as autonomous microreactors that eliminate laborious protein purification while exploiting endogenous metabolism for in situ cofactor regeneration—an intrinsic advantage inaccessible to isolated enzymes [14, 15]. However, freely suspended whole-cell systems face persistent bottlenecks for continuous bioprocessing, including limited mechanical robustness, cumbersome solid–liquid separation, and an inability to support long-term, cyclic reuse. Cell immobilization directly addresses these constraints by entrapping or anchoring strains within biocompatible matrices, thereby enhancing operational stability, simplifying downstream recovery, and enabling catalyst recyclability [16–20]. Additionally, catalytically active inclusion bodies (CatIBs) have been engineered through self-assembly as a carrier-free immobilization strategy for enzyme reuse [21]. Rational design of immobilization carriers—ranging from chitosan to sodium alginate composite hydrogels—has been shown to bolster cellular tolerance to fluctuating temperatures and pH, substantially extending catalyst service life [14]. Representative demonstrations include chitosan-entrapped *Rhodococcus pyridinivorans*, which retained robust activity at 60°C and maintained ~ 50% of initial performance over seven consecutive batches [22]. Most notably, co-immobilized dual-strain *Escherichia coli* consortia have achieved multistep biosynthesis of 4-hydroxycinnamyl alcohols from phenylpropanoic acid, validating the feasibility of immobilized, modular microbial consortia for complex pathways [23]. Similarly, spore surface-displayed enzyme cascades have been developed for multi-step cellobiose synthesis [24]. Collectively, immobilized whole-cell platforms offer a low-cost, stable, and eco-compatible route to high-value natural products. Yet, despite these advances, immobilized modular dual-strain cell factories tailored for isovitexin biosynthesis—specifically integrating dedicated C-glycosylation and autonomous cofactor-regenerating modules—remain conspicuously underexplored. Closing this gap would not

only enable green, high-efficiency production of flavone C-glycosides, but also provide standardized isovitexin sufficient to underpin rigorous pharmacological and mechanistic investigations.

Herein, we rationally design and construct a magnetically recoverable immobilized modular dual-*E. coli* microbial cell factory to achieve green, high-efficiency biosynthesis of isovitexin (Scheme 1), targeting the unmet demand of reusable cofactor-self-sufficient biocatalytic platforms for flavonoid C-glycoside production. The construction workflow is divided into three core synthetic biology modules: First, solubility engineering of three plant-derived CGTs (AbCGT, GtUF6CGT1, WjGT1) via fusion of MBP, GST and SUMO solubilizing tags is performed to relieve intracellular inclusion body accumulation, and the chassis strain with optimal soluble expression and C-glucosylation activity is screened out. Second, a complementary SuSyAc-expressing auxiliary strain is introduced to assemble a dual-strain cascade pathway, which drives continuous in situ intracellular regeneration of the expensive UDP-glucose glycosyl donor without exogenous cofactor supplementation. Third, the two functional engineered strains are co-encapsulated within Fe_3O_4 nanoparticle-reinforced sodium alginate-polyvinyl alcohol-chitosan (SA-PVA-CS) ternary composite hydrogel to prepare magnetic responsive microsphere carriers, realizing rapid magnetic separation and cyclic reuse of the whole-cell factory. We systematically characterize the catalytic conversion capacity, operational tolerance and batch-to-batch recyclability of the magnetic immobilized dual-strain cell factory under optimized reaction parameters. This study delivers a versatile synthetic biology engineering framework for scalable, sustainable industrial biomanufacturing of diverse flavonoid C-glycosides, balancing outstanding catalytic performance, long-term operational stability and low-cost catalyst recovery.

Materials and Methods

Strains, Plasmids, and Key Reagents

The genes for C-glycosyltransferases (CGTs) (AbCGT, GenBank: MN747045; GtUF6CGT1, GenBank: AB985754; WjGT1, GenBank: LC465149) and sucrose synthase (SuSyAc, GenBank: AIA55343.1) used in this study were fully codon-optimized for the translational preference of *E. coli* chassis cells to maximize intracellular soluble protein accumulation in microbial cell factory, then chemically synthesized by Sangon Biotech (Shanghai) Co., Ltd. [1, 12, 13]. All genes were cloned into the pET-28a (+) expression vector to construct standardized modular expression cassettes for synthetic biology chassis engineering. The coding sequences for solubility enhancement tags MBP, GST and SUMO were PCR-amplified from *E. coli* MG1655 genomic DNA, the pGEX-4T-1 plasmid and the pPSUMO plasmid, respectively. *E. coli* DH5α was used as the cloning strain for plasmid construction and sequencing verification, while *E. coli* BL21(DE3) served as the protein expression chassis; both strains are preserved in our laboratory strain library. All chemical reagents adopted in this work are of analytical grade, including apigenin, isovitexin reference standard, isopropyl-β-D-thiogalactopyranoside (IPTG), uridine diphosphate (UDP), sucrose, sodium alginate (SA), polyvinyl alcohol (PVA), chitosan (CS), ferrous chloride tetrahydrate, and ferric chloride hexahydrate.

Construction of Recombinant Strains

PCR amplification was performed using synthesized plasmids or genomic DNA as templates with high-fidelity DNA polymerase to guarantee the fidelity of modular fusion expression elements. For the construction of fusion protein expression vectors, the recognition and cleavage site sequence for Tobacco Etch Virus (TEV) protease (GAAAACCTGTATTTTCAGGGA) was introduced between the coding sequences of the solubility tag and the target gene through primer design, enabling tag removal after protein purification without disrupting the catalytic domain of target enzymes. The amplified gene fragments were ligated with the linearized pET-28a (+) vector using a seamless cloning kit, which facilitated rapid assembly of multi-component expression modules for microbial cell factory construction. The ligation products were transformed into *E. coli* DH5α competent cells and plated on LB agar plates containing kanamycin (100 μg/mL) for transformant screening. Positive clones were initially screened by colony PCR and restriction endonuclease double digestion. Recombinant plasmids confirmed by full-length Sanger sequencing were then transformed into the *E. coli* BL21(DE3) expression host to obtain functional catalytic chassis strains.

Protein Expression and Optimization of Conditions

Recombinant *E. coli* BL21(DE3) strains were inoculated into liquid LB medium containing the corresponding antibiotic and cultured overnight at 37°C and 200 rpm to prepare seed cultures for cell factory fermentation. The next day, the seed culture was transferred at a 1% inoculum ratio into 500 mL of fermentation medium (LB, SOB, SB, TB, or modified YM9) and grown at 37°C and 200 rpm to mid-log phase (OD_{600} ≈ 0.5), the optimal growth stage for induction of heterologous protein expression. Subsequently, IPTG was added to a final concentration of 0.01–1.0 mM, and the culture temperature was lowered to 12–28°C for an additional 20 h of low-temperature induction to mitigate inclusion body formation. After induction, the cells were harvested by refrigerated centrifugation and washed twice with pre-cooled PBS buffer (pH 8.0). A portion of the cell pellet was resuspended in protein lysis buffer and sonicated on ice (50% power, 10 s on, 10 s off) to fully release intracellular proteins. The lysate was centrifuged at 14,000 × g for 20 min at 4°C. The supernatant (soluble protein fraction) and the pellet (inclusion body fraction) were collected separately for SDS-PAGE analysis to quantify soluble heterologous protein yield of each engineered chassis. The concentration of soluble protein was quantified using the grayscale quantitative method with serially diluted BSA as standard references, and the grayscale values of protein gel bands were analyzed using ImageJ software to calculate soluble protein content per unit wet cell weight, a core indicator for evaluating the catalytic potential of whole-cell factory chassis.

Dual Whole-Cell Cascade Catalysis

The two engineered *E. coli* strains individually expressing MBP-WjGT1 glycosyltransferase and SuSyAc sucrose synthase were subjected to separate fermentation and low-temperature induction following the protein expression protocol described above. After cultivation, bacterial pellets were recovered via

refrigerated centrifugation, rinsed twice with pre-cooled PBS buffer, and reconstituted to homogeneous 10% (w/v) cell suspensions for subsequent cascade catalysis.

In accordance with the single-factor optimization scheme, the two cell suspensions were blended at varied mass ratios (MBP-WjGT1:SuSyAc ranging from 99.9:0.1 to 90:10, w/w), among which the optimal proportion of 99.5:0.5 (w/w) was selected to assemble the dual-strain whole-cell biocatalyst. A 1 mL standard catalytic reaction system was formulated in 50 mM HEPES buffer (pH 8.0), consisting of 5% (w/v) mixed whole-cell catalyst, 0.5 mM apigenin, 10 mM sucrose, and 5% (v/v) DMSO as biocompatible co-solvent to improve the solubility of hydrophobic apigenin. The bioconversion reaction was incubated at 30°C with shaking at 1000 rpm for 16 h.

To acquire the maximum apigenin conversion and isovitexin titer, key reaction parameters were sequentially optimized using a one-factor-at-a-time approach, including the mass ratio of two engineered strains, exogenous UDP dosage (0–2 mM), sucrose concentration (5–100 mM), DMSO proportion (5–30%, v/v), and initial apigenin substrate concentration (0.25–1.25 mM). All optimization groups were performed in triplicate to ensure data reproducibility.

Engineering of magnetic composite hydrogel carrier for immobilized whole-cell factory

Hydrophilic Fe_3O_4 nanoparticles were prepared by the co-precipitation method [19, 25]. $FeCl_2{\cdot}4H_2O$ and $FeCl_3{\cdot}6H_2O$ (molar ratio 1:1.75) were dissolved in a 50% ethanol-water solution. At 80°C under a nitrogen atmosphere to prevent ferrous oxidation, ammonia water was added dropwise until the pH reached 10, and the reaction was continued for 3 h. After the reaction, the magnetic nanoparticle product was collected by external magnetic separation, washed successively with ethanol-water solution and absolute ethanol, and finally dried under vacuum to obtain magnetically responsive filler for hydrogel carrier fabrication.

The preparation of the magnetic immobilized microspheres was carried out as follows. First, a homogeneous hydrogel matrix solution was prepared containing 2% (w/v) sodium alginate, 10% (w/v) PVA, 5% (w/v) CS, and 2% (w/v) Fe_3O_4 nanoparticles [18, 20, 26]. SA-PVA-CS ternary composite hydrogel was selected as immobilization matrix for its balanced mechanical strength, biocompatibility and porous mass transfer channels for substrate and product diffusion inside immobilized cell factories. Subsequently, the cell suspension (50% cell concentration, with the two cell types mixed at the optimal mass ratio) was combined with an equal volume of the matrix solution and mixed thoroughly to form a homogeneous cell-hydrogel precursor mixture. This mixture was then extruded dropwise through a syringe pump at a constant rate into a pre-chilled calcium chloride-boric acid crosslinking solution (containing 7.2 g/L $CaCl_2$ and 7.2 g/L boric acid). The droplets rapidly solidified into uniform microbeads in the crosslinking solution and were left to crosslink overnight at 4°C to complete carrier shaping. Finally, the resulting magnetic hydrogel microspheres were collected, washed several times with sterile water to remove residual crosslinker, and stored at 4°C until catalytic use.

To investigate the surface morphology and internal porous structure that determines mass transfer efficiency of the immobilized whole-cell factory, the prepared microspheres were washed thoroughly with pure water and flash-frozen in liquid nitrogen, followed by lyophilization overnight to maintain intact microscale structure. For cross-sectional observation, the freeze-dried microspheres were manually fractured to expose the internal cell embedding structure. A small amount of the sample was dispersed in ethanol and mounted on a silicon wafer using conductive tape. After natural drying, the samples were gold-sputtered for 20 s using an ion sputter coater to enhance electrical conductivity for electron imaging. The surface and cross-sectional morphologies of the microspheres, as well as the prepared Fe_3O_4 nanoparticles, were observed using a scanning electron microscope (SEM).

Catalyst Performance Assessment and Product Analysis

The activity measurement protocol for magnetic hydrogel co-immobilized dual-strain whole-cell catalysts was modified based on the C-glycosyltransferase activity assay described above, with the total reaction volume scaled up to 1 mL in 50 mM HEPES buffer. The loading amount of immobilized biocatalyst was calculated according to the mass of unimmobilized mixed cell suspension used during hydrogel preparation, ensuring identical total wet cell mass between free whole-cell control groups and immobilized catalyst groups for fair activity comparison. The reaction system incubated at 30°C and 1000 rpm. After the reaction, 4 volumes of pre-chilled methanol were immediately added to terminate biocatalysis and precipitate intracellular proteins and whole cells. The mixture was centrifuged at 14,000 rpm for 30 min. The supernatant was collected and filtered through a 0.22 μm organic phase membrane before injection for analysis. Quantitative analysis of the target biosynthetic product isovitexin was performed using a High-Performance Liquid Chromatography (HPLC) system (Agilent 1260 Infinity II). Chromatographic separation was performed on a Supersil ODS2 column (3 μm, 2.1 mm × 150 mm) with the column temperature maintained at 30°C. The mobile phase consisted of 0.1% (v/v) formic acid in water (A) and 0.1% (v/v) formic acid in acetonitrile (B), using a gradient elution at a flow rate of 0.2 mL/min. The detection wavelength was set at 340 nm. The product was identified and quantified by comparing its retention time and peak area with those of serially diluted isovitexin standard solutions. Two core performance indicators of microbial cell factory were calculated: substrate molar conversion rate and final isovitexin volumetric titer (mg/L), which were used to evaluate the catalytic capacity of free dual strains and magnetic immobilized microspheres.

To test the reusability of the immobilized magnetic cell factory, at the end of each reaction cycle (1 mL system), the reaction tube was placed in an external permanent magnetic field. Once the microspheres were completely attracted to the tube wall, the supernatant containing target product was carefully removed. Then, fresh HEPES buffer was added to wash the microspheres three times to remove residual unreacted apigenin and accumulated isovitexin. After washing, a newly prepared reaction substrate solution was added to start the next catalytic cycle, and this magnetic separation-washing-reaction cycle was repeated for seven batches to assess long-term operational stability.

Standard biosafety procedures for handling genetically modified *E. coli* strains were strictly followed throughout all experimental operations. All chemical reagents were handled according to their corresponding Material Safety Data Sheets (MSDS) to avoid toxic and corrosive hazards.

Results and Discussion

Solubility Engineering and Screening of High-Performance CGT Catalytic Chassis

Plant-derived CGTs represent the core catalytic modules for constructing flavonoid synthetic microbial cell factories. Three reported C-6 regioselective CGTs (AbCGT, GtUF6CGT1, WjGT1) were selected as candidate enzymes in this work. After codon optimization tailored to *E. coli* translational preference, target genes were chemically synthesized and assembled into pET-28a(+) vectors, followed by transformation into BL21(DE3) chassis cells. Colony PCR and double restriction digestion verified all positive recombinant strains (Figure S1 supplementary data). SDS-PAGE protein profiling revealed obvious heterologous overexpression of three CGTs, yet nearly all recombinant proteins accumulated as insoluble inclusion bodies even under mild low-temperature induction conditions, which is a universal metabolic bottleneck limiting the catalytic capacity of plant enzyme cell factories in prokaryotic hosts. Whole-cell biocatalysis quantification further confirmed this defect: unmodified WjGT strain only reached 33.0% apigenin conversion, while AbCGT and GtUF6CGT exhibited much weaker catalytic efficiency (Fig. 1b). We infer that the severe shortage of soluble folded CGT protein, rather than insufficient gene transcription, is the root cause of low biotransformation activity.

To break the inclusion body barrier and improve intracellular functional protein abundance, three classic solubility-enhancing fusion tags (MBP, GST, SUMO) were separately fused to the N-terminus of each CGT coding sequence. A TEV protease cleavage site was inserted between tag and catalytic domain to realize complete tag removal after purification without destroying enzyme active center structure, forming nine combinatorial fusion expression constructs. Small-scale shake-flask expression screening (Fig. 1c) visually verified that all three fusion tags significantly raised the soluble protein proportion of CGTs. Quantitative normalization of soluble protein content by unit wet cell weight (Fig. 1d) proved MBP tag possessed the strongest solubilization effect for all three enzymes, and MBP-WjGT1 achieved 245 μg/mg soluble protein under unoptimized fermentation conditions. To exclude tag interference on intrinsic catalytic activity, all fusion proteins and tag-free purified CGTs were standardized to identical molar concentrations for activity testing (Fig. 1e). The results indicated fusion tags only imposed negligible inhibitory effects on CGT glucosylation capacity, and MBP-WjGT1 delivered the highest apigenin conversion rate up to 98.3% (Figure S2), thus being screened as the core catalytic chassis strain for subsequent cascade construction.

Molecular mechanism underlying MBP-mediated solubility enhancement can be preliminarily interpreted by protein structural characteristics, consistent with previous enzyme structural analysis reported in Nallamsetty & Waugh (2007) [27]. The MBP tag possesses a large hydrophilic *β*-barrel outer domain that acts as a molecular chaperone: it shields the hydrophobic aggregation-prone interface of plant-derived CGTs exposed during nascent polypeptide folding in *E. coli* cytoplasm, weakens inter-molecular hydrophobic interactions between unfolded CGT monomers, and restrains spontaneous self-assembly into insoluble inclusion bodies. In contrast, GST and SUMO only provide limited hydrophilic surface area, resulting in weaker anti-aggregation capacity. This spatial shielding effect of the MBP domain directly elevates the proportion of correctly folded catalytic domains available for apigenin glucosylation, fundamentally boosting the intrinsic catalytic flux of the single-strain cell factory chassis.

Further multi-factor fermentation engineering optimization was carried out to maximize soluble expression of MBP-WjGT1 (Figure S3). Medium type, IPTG dosage and post-induction temperature were systematically adjusted, and the optimal culture regime was confirmed as SOB medium cultured to OD_{600} ≈ 0.5, induced by 0.5 mM IPTG at 16°C for 20 h. Under this optimized fermentation module, intracellular soluble MBP-WjGT1 content was further lifted to 374.0 μg/mg wet cell, laying a high-efficiency catalytic foundation for dual-strain cofactor self-circulation cell factory assembly.

Construction and Biochemical Characterization of SuSyAc Cofactor Regeneration Module

The single MBP-WjGT1 chassis relies on expensive exogenous UDP-glucose as glycosyl donor, which greatly increases raw material cost and restricts the industrial scalability of mono-strain biocatalysis. To build a self-sufficient cofactor circulation pathway inside intact cells, we constructed an independent auxiliary chassis strain expressing *Acidithiobacillus caldus*-derived sucrose synthase SuSyAc as the second functional module of the dual-strain cell factory.

The SuSyAc coding sequence was cloned into pET-28a(+) vector and transformed into BL21(DE3). After auto-induction culture using pET-Lac medium, total protein expression profile was detected (Figure S4). Purified SuSyAc protein was quantified by BCA method and subjected to enzyme activity assay, with measured specific activity reaching 15.4 U/mg, sufficient to drive continuous UDP-glucose regeneration coupled with the CGT catalytic reaction. This cofactor regeneration strain can supply UDP-Glc via sucrose decomposition without expensive cofactor feeding, eliminating the core economic defect of single-enzyme/single-strain catalytic systems. The two engineered strains respectively undertake glucosylation and cofactor recycling functions, laying the foundation for modular dual-strain cascade biocatalysis.

Single-Factor Optimization of Free Dual-Strain Cascade Catalytic System

We mixed MBP-WjGT1 catalytic cells and SuSyAc cofactor-regenerating cells to assemble a two-component whole-cell microbial cell factory, and optimized all key reaction parameters one-factor-at-a-time to maximize apigenin conversion and isovitexin titer. First, comparison between mono-strain and dual-strain systems (Fig. 2a): single MBP-WjGT1 strain supplemented with UDP-Glc achieved 99.0% conversion, while the dual-strain system replacing expensive UDP-Glc with cheaper UDP maintained a comparable 98.5% conversion rate, demonstrating the metabolic compatibility and functional synergy of the two modular strains. Next, the mass ratio of two cell types was tuned (Fig. 2b). The system reached peak activity at MBP-WjGT1 : SuSyAc = 99.5 : 0.5 (w/w). Too little SuSyAc cells caused insufficient UDP-Glc flux; excessive auxiliary strains diluted catalytic cell density and reduced overall reaction efficiency, which revealed only a tiny proportion of regeneration module could satisfy the demand of glucosylation reaction.

Subsequent exogenous UDP gradient experiments brought a critical discovery (Fig. 2c): the reaction group without any external UDP addition exhibited the highest conversion efficiency. It demonstrated endogenous UDP produced by *E. coli* central carbon metabolism can fully support closed-loop UDP-Glc circulation, completely removing the input cost of expensive UDP raw materials and forming a prominent economic advantage over reported cell-free enzyme

cascades. Sucrose concentration optimization (Fig. 2d) showed 10 mM was optimal; low sucrose limited cofactor regeneration, while high concentration triggered substrate competitive inhibition and osmotic pressure damage to intracellular enzymes. The self-sufficient UDP supply without exogenous addition originates from central carbon metabolism of *E. coli* chassis cells. Endogenous UDP is continuously generated via the glycolysis-pentose phosphate coupled pathway: intracellular glucose-6-phosphate and glucose-1-phosphate are converted into UTP through nucleotide de novo synthesis, then UTP reacts with glucose-1-phosphate under SuSyAc catalysis to form UDP-glucose for glucosylation; the phosphate and UDP released after CGT-mediated glycosylation re-enter the nucleotide metabolic pool to realize closed-loop circulation. Unlike cell-free systems that require constant external UDP supplementation, the complete intracellular metabolic network of whole-cell factories forms a spontaneous cofactor cycle pipeline, eliminating the need for artificial cofactor feeding.

Apigenin has extremely low water solubility, so DMSO was selected as biocompatible co-solvent (Fig. 2e). 5% (v/v) DMSO realized maximum conversion; higher concentrations destroyed cell membrane integrity and denatured both intracellular CGT and SuSyAc, leading to sharp activity loss. Finally, substrate concentration gradient and time-course kinetic experiments (Fig. 2f, 2g) were performed under all fixed optimal conditions. 0.5 mM apigenin obtained 98.5% conversion within 16 h; raising substrate to 1.25 mM reached a plateau titer of 0.46 mM (212.6 mg/L isovitexin) with 98.0% molar conversion, which defined the baseline productivity of suspended free dual-strain cell factory.

Ternary SA-PVA-CS Hydrogel Carrier Formulation Optimization and Microstructural Analysis

Free whole-cell catalysts suffer poor mechanical strength and difficult solid-liquid separation, which cannot meet the demand of cyclic industrial bioproduction. We adopted sodium alginate-polyvinyl alcohol-chitosan (SA-PVA-CS) ternary composite hydrogel as immobilization carrier, and optimized carrier composition to balance catalytic activity and mechanical durability, followed by SEM microstructural characterization to interpret mass transfer characteristics.

Initial carrier formula (2% SA, 5% PVA, 5% CS) co-immobilized dual strains and achieved 91.0% apigenin conversion, retaining 92.9% activity of free cells (Fig. 3a). However, the microspheres only preserved 40.3% initial activity after seven batches, proving the carrier formula needed further tuning. Single-factor adjustment of chitosan and PVA content was carried out separately: varying chitosan concentration barely affected catalytic performance (Fig. 3b), because CS mainly acts as crosslinker without changing internal pore channels. In contrast, PVA concentration dominated hydrogel porosity and mass transfer resistance (Fig. 3c). When PVA rose to 10% (w/v), conversion still maintained 84.0%; further PVA addition shrank pore size and aggravated substrate diffusion limitation, reducing conversion efficiency. Reusability test of 10% PVA optimized microspheres (Fig. 3d) showed significantly improved multi-batch stability compared with 5% PVA formulation, realizing a better trade-off between mechanical toughness and substrate permeability.

SEM imaging was adopted to analyze microsphere structure (Fig. 3e, f). Surface SEM presented interconnected sponge-like porous networks that provide unobstructed diffusion channels for apigenin, sucrose and target product; cross-section images clearly displayed uniform embedding of two engineered *E. coli* strains inside the three-dimensional hydrogel matrix, verifying successful co-immobilization of both catalytic and cofactor-regenerating modules. The optimized carrier formula (2% SA, 10% PVA, 5% CS) was selected for subsequent magnetic modification experiments. The sponge-like porous network captured via SEM governs substrate diffusion kinetics within immobilized whole-cell factories. Interconnected micron-sized pores act as mass transfer corridors for both hydrophobic apigenin-DMSO complexes and water-soluble sucrose and UDP intermediates. Higher PVA loading compresses pore dimensions and raises matrix tortuosity, lengthening substrate transport pathways and creating internal concentration gradients within hydrogel beads, which accounts for the gradual drop in bioconversion activity under excessive PVA concentrations. The optimized 10% PVA formulation strikes a favorable balance between robust mechanical crosslinking and unimpeded substrate diffusion rates, maximizing the comprehensive catalytic capacity of this solid-state biocatalytic platform.

Fabrication and Cyclic Stability Evaluation of Magnetic Immobilized Cell Factory

To realize rapid, low-cost catalyst recovery without centrifugation/filtration operations, Fe_3O_4 hydrophilic magnetic nanoparticles were synthesized via co-precipitation and blended into the optimized SA-PVA-CS hydrogel matrix to prepare magnetically responsive immobilized microspheres *E. coli*@SA-PVA-CS-Fe_3O_4. SEM characterization of pure Fe_3O_4 nanoparticles (Fig. 4a) displayed uniform particle size and good aqueous dispersibility; macroscopic observation confirmed the microspheres could be rapidly separated under external magnetic field (Fig. 4b), realizing convenient catalyst recycling. Catalytic performance and cyclic reusability of magnetic hydrogel microspheres were systematically assessed (Fig. 4c). The magnetic immobilized cell factory delivered 80.0% substrate conversion (81.6% relative activity vs free dual strains), the slight activity decline originated from extra mass transfer barrier introduced by magnetic nanoparticles inside hydrogel pores. More importantly, after seven consecutive magnetic separation-reaction cycles, the microspheres still retained 64.0% initial catalytic conversion capacity. Compared with non-magnetic hydrogel carriers, magnetic modification simplified downstream separation process without seriously sacrificing long-term operational stability, solving two core engineering bottlenecks of free whole-cell catalysts: hard recovery and single use. This magnetic co-immobilization strategy provides a recyclable solid-state chassis for continuous flavonoid C-glycoside biosynthesis. The gradual loss of catalytic activity over seven successive magnetic separation cycles stems from three interrelated microscale mechanisms: (1) Intact cell leakage: repeated stirring and buffer rinsing cause mild swelling of the hydrogel network, which triggers partial detachment of surface-trapped *E. coli* cells into the liquid phase; (2) internal pore clogging: hydrophobic isovitexin products and tiny cellular residues accumulate within porous channels, raising mass transfer barriers and limiting substrate delivery to intracellular catalytic enzymes; (3) intracellular proteolytic degradation: prolonged incubation at 45°C moderately activates endogenous proteases inside encapsulated bacterial cells, which slowly break down folded CGT and SuSyAc proteins and reduce the total pool of functional biocatalysts. Carrier swelling and concomitant cell leakage represent the primary contributor to performance decline across repeated reaction batches.

Quantitative Benchmarking with Reported Biocatalytic Cell Factory Platforms

To comprehensively evaluate the industrial translation potential of our magnetically recyclable modular dual-strain microbial cell factory, we performed a multi-dimensional quantitative benchmark against representative cell-free and whole-cell biocatalytic platforms documented in previous studies (Table 1). Beyond conventional metrics including substrate conversion, catalyst reusability and mandatory protein purification procedures, two critical industrial economic indicators—total preparation labor time and relative raw material consumption per unit reaction—were newly incorporated into the comparative framework to deliver a full-scale cost-benefit assessment.

Table 1
Comparison of biocatalytic systems for preparation of apigenin C-glycosides

Catalyst System	Catalyst Form	Catalytic Route	Molar conversion(%)	Reusability (batch / residual activity)	Purification procedure required	Total preparation labor time	Relative raw material cost (Unit reaction)	Reference
Gt6CGT + GmSUS	Purified free enzyme cascade	Cell-free one-pot apigenin glucosylation	97.10	Single-use (1 cycle only)	Yes (Ni-NTA affinity chromatography, cell lysis + multi-step desalting)	Long (≥ 24 h strain culture + ≥ 12 h protein purification)	Extremely high (large dosage expensive UDP-Glc + chromatographic resin consumption)	[12]
TcCGT + GmSUS	Purified free enzyme cascade	Cell-free one-pot apigenin glucosylation	97.30	Single-use (1 cycle only)	Yes (Ni-NTA affinity purification)	Long (≥ 24 h culture + 10 h enzyme isolation)	Extremely high (exogenous UDP supplement & chromatographic consumables)	[13]
Free dual E. coli whole cells (CGT + SuSyAc)	Suspended whole-cell biocatalyst	Free dual-strain cascade, endogenous UDP circulation	94–97	Single-use, difficult solid-liquid separation	No enzyme purification, but two separate fermentation batches	Medium (16 h dual strain cultivation, no purification step)	Medium (only sucrose as sacrificial substrate, no exogenous UDP)	[12]
Co-immobilized single-strain E. coli (Phenylpropanoid pathway)	Non-magnetic SA-PVA immobilized whole cell	Single strain multi-step cascade	ND	7 cycles / ~50% residual activity	No protein purification	Medium (18 h culture + 4 h hydrogel embedding)	Medium-low (only simple carbon source feeding)	[23]
MBP-WjGT1 + SuSyAc co-immobilized E. coli@SA-PVA-CS-Fe_3O_4	Magnetically recyclable composite hydrogel immobilized modular dual-strain microbial cell factory	Modular dual-strain cascade with full endogenous UDP-Glc in-situ regeneration	98.50	7 consecutive cycles / 64% initial conversion retained	Zero enzyme purification, one-step co-immobilization after mixed cell collection	Medium-short (16 h dual strain fermentation + 3 h magnetic hydrogel microsphere preparation)	Lowest (UDP-free, low-dose sucrose, recyclable magnetic carrier reusable for multiple batches)	This work
Note:								
1. Total preparation labor time classification standard								
• Long: ≥36 h total workflow including microbial culture, cell lysis and chromatographic protein purification;								
• Medium: 16–24 h, dual strain fermentation without protein isolation;								
• Medium-short: Integrated cell mixing and one-step magnetic carrier embedding, no repeated carrier fabrication per batch.								
2. Relative raw material cost grading standard (based on 1 mL standard catalytic reaction system)								
• Extremely high: Require continuous supplementation of expensive UDP/UDP-glucose, consume disposable chromatographic filler in each batch;								
• Medium: No enzyme purification consumables, but catalyst cannot be recycled, strains need repeated culture for every reaction batch;								
• Lowest: No exogenous expensive cofactor input, magnetic hydrogel microspheres can be recovered magnetically and reused repeatedly, cutting repeated strain cultivation and carrier manufacturing cost for long-term bioproduction.								
3. ND = Not determined in original literature.								

Reported cell-free cascade systems constructed with purified CGT and sucrose synthase pairs, such as the platforms developed by Pei et al. and Qiu et al., can achieve extremely high fed-batch volumetric titers reaching 3772 mg/L and 5050 mg/L of target flavonoid C-glycosides respectively. Nevertheless, such systems carry prohibitive industrial barriers: they demand lengthy workflows of cell lysis and multi-round Ni-NTA affinity chromatographic separation to harvest pure enzymes, accompanied by single-use catalyst characteristics. As summarized in Table 1, these free enzyme workflows require extremely long total preparation labor time and incur exorbitant raw material expenditures driven by continuous exogenous UDP supplementation and disposable chromatographic media consumption.

Although our single-batch isovitexin titer (212.6 mg/L) is lower than the fed-batch outputs of purified enzyme cascades, this gap originates merely from mass transfer resistance imposed by the hydrogel matrix on poorly water-soluble apigenin, rather than insufficient intrinsic catalytic capacity of the

engineered strain chassis. The core competitive strengths of our immobilized cell factory manifest in drastically cut preparation labor and minimized long-term raw material outlay, paired with recyclable catalytic performance. Only two parallel seed fermentations are required without any protein purification steps, and the integrated cell embedding procedure shortens total preparation labor to a medium-short cycle. Meanwhile, the endogenous UDP circulation pathway completely eliminates expensive external cofactor inputs, and magnetic microspheres can be repeatedly recovered for multiple reaction runs, resulting in the lowest relative raw material cost among all compared biocatalytic schemes.

Over seven successive magnetic recycling batches, the cumulative isovitexin yield approaches 900 mg/L. When accounting for recurring labor and reagent expenses associated with enzyme purification required by disposable free enzyme systems, the overall economic efficiency of our recyclable cell factory becomes distinctly competitive. Preliminary fed-batch feeding trials with four sequential 0.25 mM apigenin supplements yielded isovitexin titers exceeding 400 mg/L with no observable catalytic attenuation, demonstrating that rational substrate feeding tactics can further lift volumetric productivity. Follow-up optimization strategies will focus on fabricating high-permeability porous hydrogel carriers to mitigate internal diffusion limitations, as well as integrating complete de novo apigenin biosynthetic pathways into the dual-strain chassis to realize one-pot synthesis from cheap simple carbon feedstocks. Collectively, this magnetically recoverable modular dual-strain microbial cell factory strikes an optimal balance between catalytic efficiency, multi-batch operational durability and industrial economic viability, establishing a cost-effective sustainable engineering blueprint for large-scale green manufacturing of diverse flavonoid C-glycosides.

Conclusion

Here, we report the rational construction of a modular, magnetically recoverable dual-*E. coli* cell factory for the green, one-pot biosynthesis of isovitexin. By implementing systematic solubility engineering using MBP, GST, and SUMO fusion tags, we overcame the notorious inclusion body formation typically associated with heterologous expression of plant-derived CGTs, identifying MBP-WjGT1 as the optimal catalytic module with a soluble expression yield of 374.0 μg/mg wet cell weight and a 98.3% apigenin conversion rate. To circumvent the economic barrier of exogenous UDP-glucose supplementation, we engineered a complementary SuSyAc-expressing auxiliary strain, establishing a synergistic consortium that facilitates autonomous, in vivo UDP-glucose regeneration. Under optimized stoichiometry (99.5:0.5, w/w), this cofactor-self-sufficient system achieved a 98.5% molar conversion to isovitexin (212.6 mg/L) without requiring external cofactor input. To address the limited operational stability of suspended cells, we fabricated a robust, magnetically responsive biocatalyst by co-immobilizing both strains within Fe_3O_4-functionalized SA-PVA-CS ternary hydrogel beads. This immobilized platform retained 80% of the free-cell activity and, crucially, maintained 64% of its initial conversion efficiency over seven consecutive reaction-separation cycles, significantly de-risking the catalyst cost for continuous bioprocessing. Beyond isovitexin, this modular architecture provides a versatile framework for synthesizing diverse high-value flavonoid C-glycosides. Future efforts will focus on genome-scale chassis integration—specifically, incorporating the de novo apigenin biosynthetic pathway to enable direct conversion from simple carbon sources—and refining mixed-culture fermentation protocols to streamline upstream processing, thereby further enhancing the economic viability of this platform for industrial translation.

Declarations

Acknowledgements

This work was financially supported by National Natural Science Foundation of China (Grant No. 3210120332), Natural Science Foundation of Hebei Province (Grant No. B2024201056), Innovation Team of Green Synthesis for Drug Precursors (IT2023B01), Key Laboratory of Chemical Biology of Hebei Province (22567632H), Hebei Key Laboratory of Analytical Science and Technology (22567620H).

Author Contributions

Shuangqing Fu: Conceptualization, Methodology, Validation, Formal analysis, Data curation, Writing – original draft.

Chao Zhang: Methodology, Data curation, Visualization.

Shuo Ma: Methodology, Investigation.

Yujie Yuan: Methodology, Data curation, Formal analysis.

Wei Li: Conceptualization, Resources, Funding acquisition, Writing – review & editing, Supervision.

Honglei Zhang: Conceptualization, Resources, Funding acquisition, Formal analysis, Writing – review & editing, Supervision.

Conflicts of interest

There are no conflicts of interest to disclose.

Data Availability

ll raw and processed experimental data supporting the findings of this study are included within the manuscript and its supplementary information files, including SDS-PAGE images, HPLC chromatograms, quantitative catalytic performance data, scanning electron microscopy photographs, and single-factor optimization curves. The gene sequences of AbCGT, GtUF6CGT1, WjGT1 and SuSyAc referenced in this work are publicly available from the GenBank

database under accession numbers MN747045, AB985754, LC465149 and AIA55343.1, respectively. All engineered strains and plasmids constructed in this study are available from the corresponding authors upon reasonable request.

References

1. Zhang YQ, Zhang M, Wang ZL, Qiao X, Ye M. Advances in plant-derived C-glycosides: Phytochemistry, bioactivities, and biotechnological production. Biotechnol Adv. 2022;60:108030.
2. Zhou Z, Li J, Zhang X. Natural flavonoids and ferroptosis: potential therapeutic opportunities for human diseases. J Agric Food Chem. 2023;71:5902–16.
3. Kumar S, Pandey AK. Chemistry and biological activities of flavonoids: an overview. Sci world J. 2013;2013:162750.
4. Roy A, Khan A, Ahmad I, Alghamdi S, Rajab BS, Babalghith AO, Alshahrani MY, Islam S, Islam MR. Flavonoids a bioactive compound from medicinal plants and its therapeutic applications. *BioMed research international* 2022, 2022:5445291.
5. Tao M, Li R, Xu T, Zhang Z, Zheng D, Xia Z, Wu T, Pan S, Xu X. Vitexin and isovitexin delayed ageing and enhanced stress-resistance through the activation of the SKN-1/Nrf2 signaling pathway. Int J Food Sci Nutr. 2023;74:685–94.
6. Yutharaksanukul P, Tangpromphan P, Tunsagool P, Sae-Tan S, Nitisinprasert S, Somnuk S, Nakphaichit M, Pusuntisumpun N, Wanikorn B. Effects of purified vitexin and Iso-Vitexin from mung bean seed coat on anti-hyperglycemic activity and gut microbiota in overweight individuals' modulation. Nutrients. 2024;16:3017.
7. Ayuni D, Devahastin S, Sirikantaramas S, Neri L, Pittia P, Pattarapipatkul N, Borompichaichartkul C. Extraction methods comparison and optimization for isoorientin and isovitexin from Thai jasmine rice leaves. J Food Meas Charact. 2024;18:9423–34.
8. Plaza M, Turner C. Pressurized hot water extraction of bioactives. TRAC Trends Anal Chem. 2015;71:39–54.
9. De Rodríguez SL, Ramírez-Garza R, Serna Saldívar SO. Environmentally friendly methods for flavonoid extraction from plant material: Impact of their operating conditions on yield and antioxidant properties. *The Scientific World Journal* 2020, 2020:6792069.
10. Gutmann A, Lepak A, Diricks M, Desmet T, Nidetzky B. Glycosyltransferase cascades for natural product glycosylation: Use of plant instead of bacterial sucrose synthases improves the UDP-glucose recycling from sucrose and UDP. Biotechnol J. 2017;12:1600557.
11. Schmölzer K, Lemmerer M, Nidetzky B. Glycosyltransferase cascades made fit for chemical production: Integrated biocatalytic process for the natural polyphenol C-glucoside nothofagin. Biotechnol Bioeng. 2018;115:146–57.
12. Pei J, Sun Q, Gu N, Zhao L, Fang X, Tang F, Cao F. Production of isoorientin and isovitexin from luteolin and apigenin using coupled catalysis of glycosyltransferase and sucrose synthase. Appl Biochem Biotechnol. 2020;190:601–15.
13. Qiu C, Wang H, Zhao L, Pei J. Orientin and vitexin production by a one-pot enzymatic cascade of a glycosyltransferase and sucrose synthase. Bioorg Chem. 2021;112:104926.
14. Polakovič M, Švitel J, Bučko M, Filip J, Neděla V, Ansorge-Schumacher MB, Gemeiner P. Progress in biocatalysis with immobilized viable whole cells: systems development, reaction engineering and applications. Biotechnol Lett. 2017;39:667–83.
15. Ricca E, Brucher B, Schrittwieser JH. Multi-enzymatic cascade reactions: overview and perspectives. Adv Synth Catal. 2011;353:2239–62.
16. Cui C, Ming H, Li L, Li M, Gao J, Han T, Wang Y. Fabrication of an in-situ co-immobilized enzyme in mesoporous silica for synthesizing GSH with ATP regeneration. Mol Catal. 2020;486:110870.
17. Nasution H, Harahap H, Dalimunthe NF, Ginting MHS, Jaafar M, Tan OO, Aruan HK, Herfananda AL. Hydrogel and effects of crosslinking agent on cellulose-based hydrogels: A review. Gels. 2022;8:568.
18. Bai Y, Wu W. The neutral protease immobilization: Physical characterization of sodium alginate-chitosan gel beads. Appl Biochem Biotechnol. 2022;194:2269–83.
19. Fan XM, Shen JJ, Xu YY, Gao J, Zhang YW. Metabolic integration of azide functionalized glycan on *Escherichia coli* cell surface for specific covalent immobilization onto magnetic nanoparticles with click chemistry. Bioresour Technol. 2021;324:124689.
20. Huang J, Qiao C, Wang X, Gao Y, Zhao J, Luo H, Wang Y, Hou C, Huo D. The microsphere of sodium alginate-chitosan-Pichia kudriavzevii enhanced esterase activity to increase the content of esters in Baijiu solid-state fermentation. Food Chem. 2023;407:135154.
21. Romero-Martínez D, Gasteazoro F, Cofas-Vargas LF, García–Hernández E, González-Davis O, Zavala G, Rosiles-Becerril D, Vazquez-Duhalt R. Trujillo–Roldán MA, Valdez–Cruz NA: Catalytically active inclusion bodies of Bacillus clausii laccase protein recombinantly produced in E. coli for dye decolorization. Microb Cell Fact. 2026;25:95.
22. Jyoti, Bhatia K, Chauhan K, Attri C, Seth A. Improving stability and reusability of Rhodococcus pyridinivorans NIT-36 nitrilase by whole cell immobilization using chitosan. Int J Biol Macromol. 2017;103:8–15.
23. Liu S, Liu J, Hou J, Chao N, Gai Y, Jiang X. Three steps in one pot: biosynthesis of 4-hydroxycinnamyl alcohols using immobilized whole cells of two genetically engineered Escherichia coli strains. Microb Cell Fact. 2017;16:104.
24. Spannenkrebs JB, Klau LJ, Karava M, Aachmann FL, Kabisch J. Spore immobilized enzymes for the multi-step synthesis of cellobiose. Microb Cell Fact. 2026;25:43.
25. Govan J, Gun'ko YK. Recent advances in the application of magnetic nanoparticles as a support for homogeneous catalysts. Nanomaterials. 2014;4:222–41.
26. Niknezhad SV, Asadollahi MA, Zamani A, Biria D. Production of xanthan gum by free and immobilized cells of Xanthomonas campestris and Xanthomonas pelargonii. Int J Biol Macromol. 2016;82:751–6.

27. Nallamsetty S, Waugh DS. Mutations that alter the equilibrium between open and closed conformations of Escherichia coli maltose-binding protein impede its ability to enhance the solubility of passenger proteins. Biochem Biophys Res Commun. 2007;364:639–44.

Scheme

Scheme 1 is available in the Supplementary Files section.

Figures

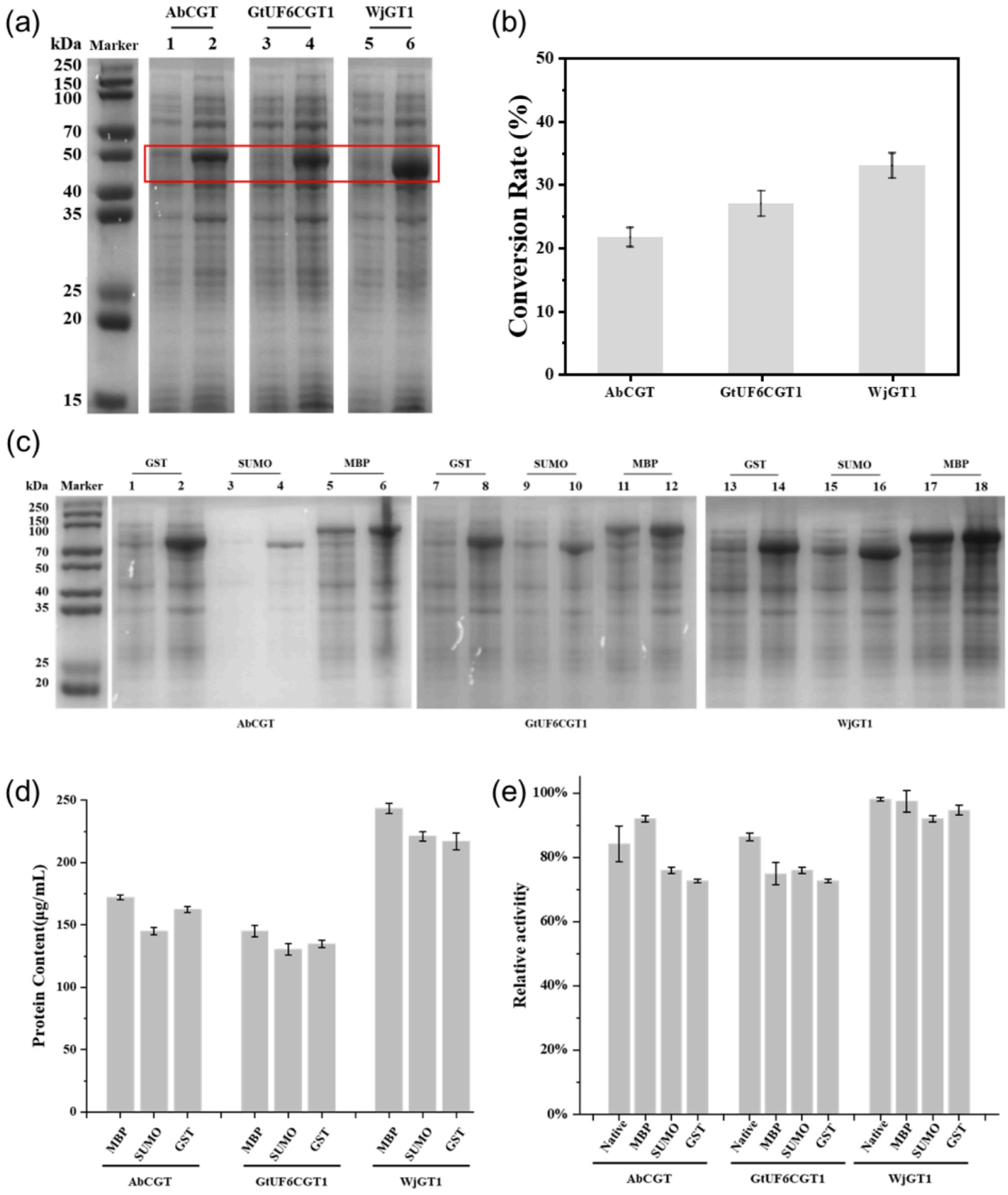


Figure 1

Screening and soluble expression optimization of CGT. (a) SDS-PAGE analysis of the initial expression of three CGT (AbCGT, GtUF6CGT1, WjGT1) in *E. coli* BL21(DE3). (b) Comparison of apigenin conversion rates using whole-cell catalysts expressing the three original CGT. (c) SDS-PAGE analysis of CGT fused with different solubility-enhancing tags (GST, SUMO, MBP). (d) Quantitative analysis of soluble protein content per unit wet cell weight for the different fusion proteins. (e) Comparison of the relative catalytic activity of fusion proteins and tag-free proteins. Data are presented as mean ± SD (n = 3).

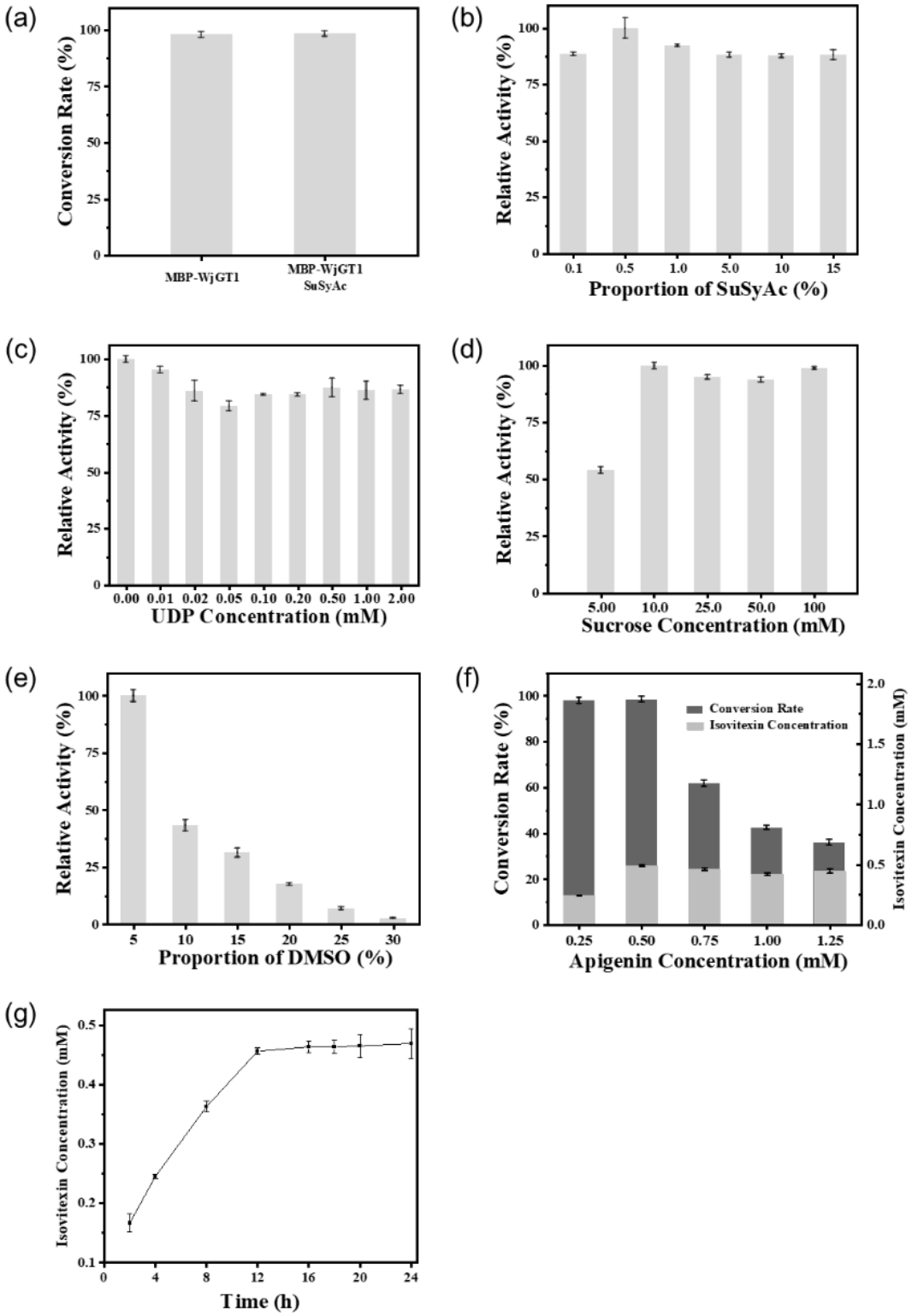


Figure 2

Optimization of reaction conditions for the dual whole-cell cascade catalytic system. (a) Comparison of conversion rates between the MBP-WjGT1 single-cell system and the dual-cell cascade system (MBP-WjGT1 + SuSyAc). (b) Effect of the proportion of SuSyAc cells in the total catalyst mass on relative activity. (c) Effect of UDP concentration on relative activity. (d) Optimization of initial sucrose concentration. (e) Effect of DMSO concentration (v/v) on the relative

activity of the system. (f) Effect of substrate (apigenin) concentration on conversion rate and isovitexin titer. (g) Time-course profile of isovitexin synthesis under optimal conditions. Data are presented as mean ± SD (n = 3).

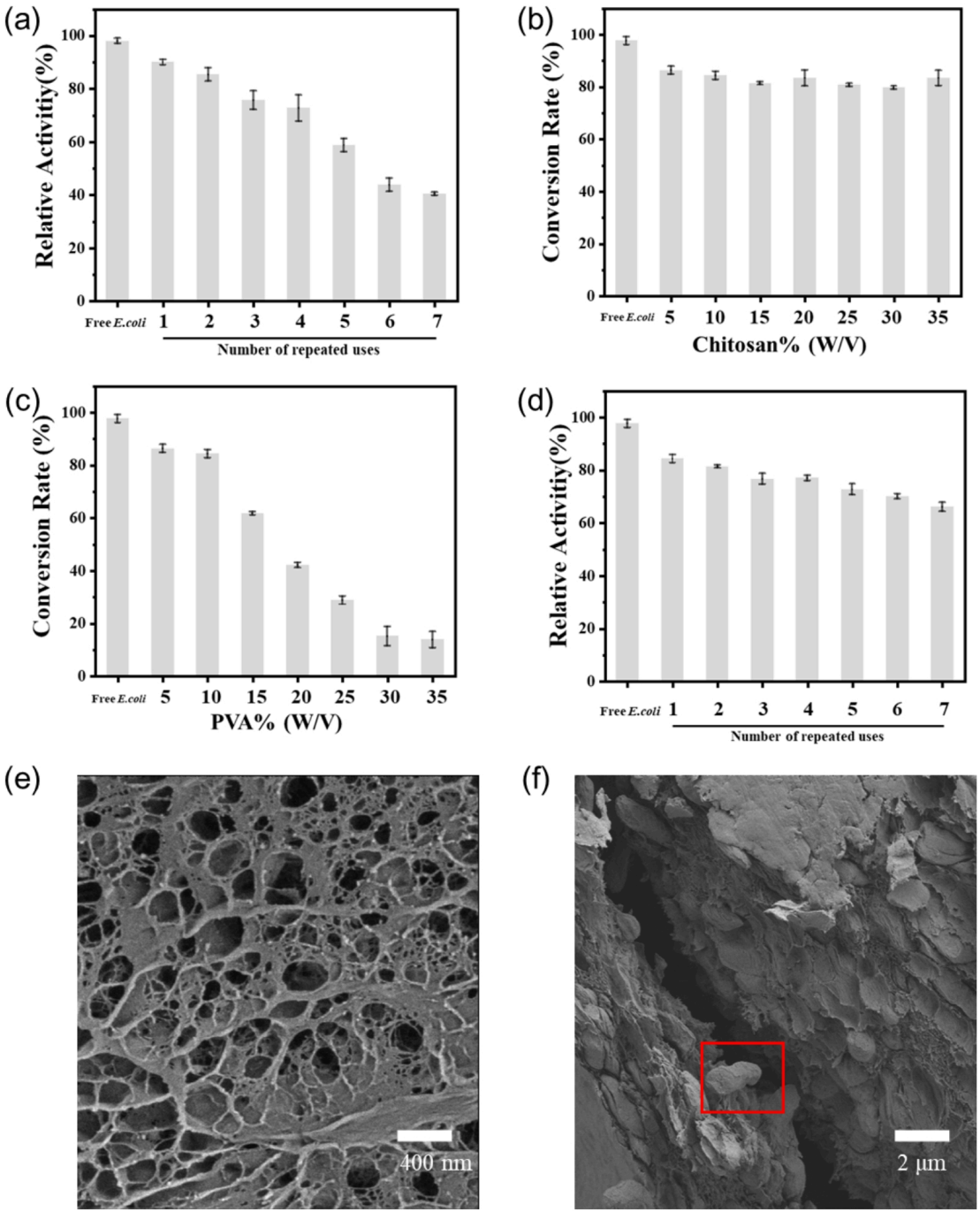


Figure 3

Optimization and characterization of the immobilized whole-cell catalyst hydrogel microspheres. (a) Reusability of the initial *E.coli*@SA-PVA-CS microspheres over 7 cycles. (b) Effect of CS concentration on the conversion rate. (c) Effect of PVA concentration on the conversion rate. (d) Reusability of the optimized *E.coli*@SA-PVA-CS (10% PVA) microspheres. (e) SEM image of the surface morphology of the optimized microspheres. (f) Cross-sectional SEM image showing *E. coli* cells immobilized within the hydrogel matrix. Data are presented as mean ± SD (n = 3).

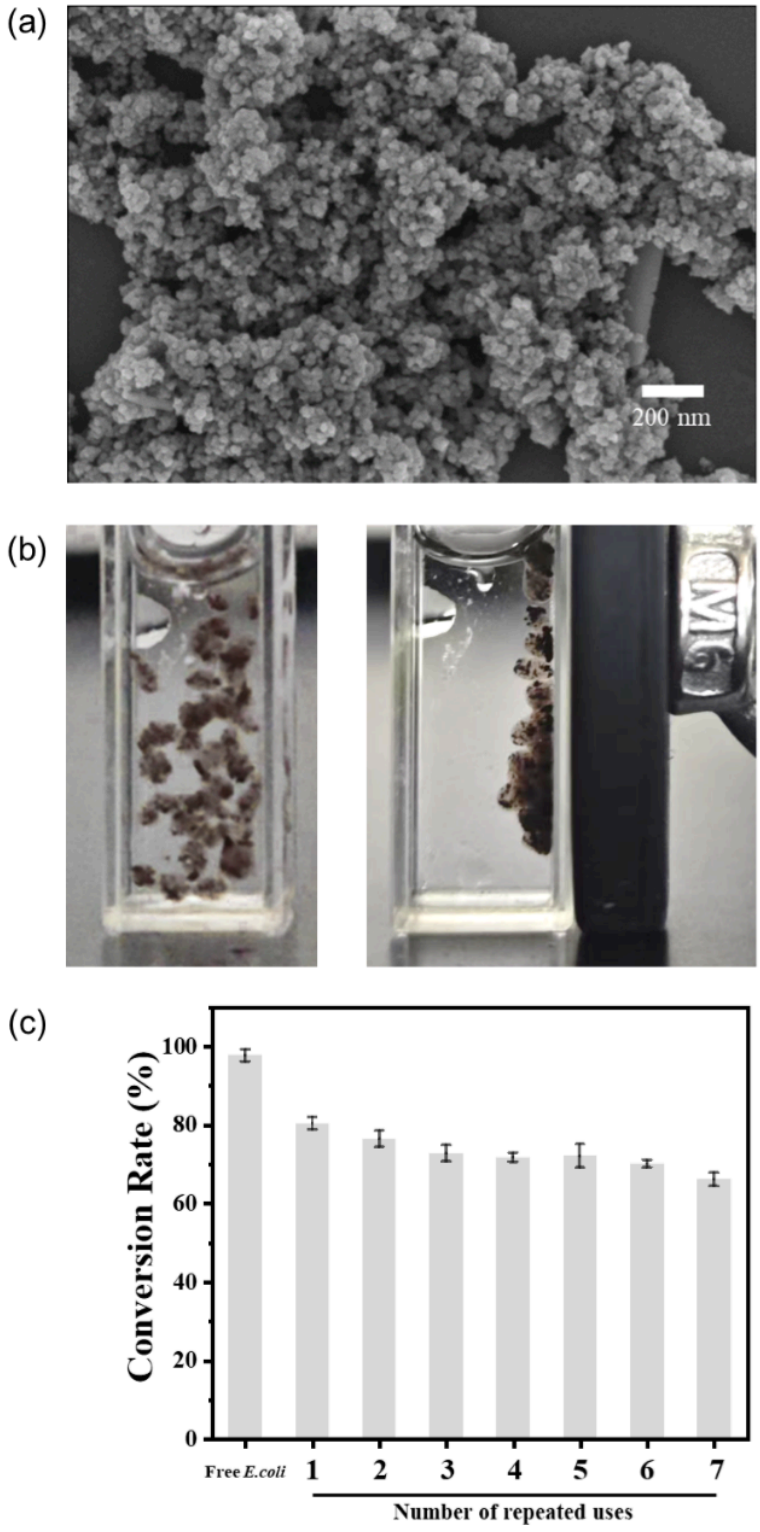


Figure 4

Characterization and performance of the magnetically responsive immobilized catalyst (*E.coli*@SA-PVA-CS-Fe_3O_4). (a) SEM image of the prepared hydrophilic Fe_3O_4 nanoparticles. (b) Photographs demonstrating the magnetic separation capability of the *E.coli*@SA-PVA-CS-Fe_3O_4 microspheres under an external magnetic field. (c) Reusability of the magnetic immobilized whole-cell catalyst over 7 consecutive reaction cycles. Data are presented as mean ± SD (n = 3).

Supplementary Files

This is a list of supplementary files associated with this preprint. Click to download.

- supportinginformation.docx

- floatimage1.jpeg